Published in final edited form as:

Eur J Neurosci. 2013 July ; 38(1): 2139–2152. doi:10.1111/ejn.12168.

Transcriptome profiling of hippocampal CA1 after early-life seizure-induced preconditioning may elucidate new genetic therapies for epilepsy

L. K. Friedman[1,2], **J. Mancuso**[2], **A. Patel**[2], **V. Kudur**[2], **J. R. Leheste**[2], **S. Iacobas**[3], **J. Botta**[3], **D. A. Iacobas**[3], and **D. C. Spray**[3]

[1]Basic Sciences, Cell Biology & Anatomy, New York Medical College, 50 Dana Rd, Valhalla, NY, 10595, USA

[2]Neuroscience, New York College of Osteopathic Medicine/New York Institute of Technology, College of Osteopathic Medicine, NY 11568, USA

[3]Albert Einstein College of Medicine, Bronx, NY 10461, USA

Abstract

Injury of the CA1 subregion induced by a single injection of kainic acid (1 × KA) in juvenile animals (P20) is attenuated in animals with two prior sustained neonatal seizures on P6 and P9. To identify gene candidates involved in the spatially protective effects produced by early-life conditioning seizures we profiled and compared the transcriptomes of CA1 subregions from control, 1 × KA- and 3 × KA-treated animals. More genes were regulated following 3 × KA (9.6%) than after 1 × KA (7.1%). Following 1 × KA, genes supporting oxidative stress, growth, development, inflammation and neurotransmission were upregulated (e.g. Cacng1, Nadsyn1, Kcng1, Aven, S100a4, GFAP, Vim, Hrsp12 and *Grik1*). After 3 × KA, protective genes were differentially over-expressed [e.g. *Cat*, *Gpx7*, *Gad1*, *Hspa12A*, *Foxn1*, adenosine A1 receptor, Ca^{2+} adaptor and homeostasis proteins, *Cacnb4*, *Atp2b2*, anti-apoptotic *Bcl-2* gene members, intracellular trafficking protein, *Grasp* and suppressor of cytokine signaling (*Socs3*)]. Distinct anti-inflammatory interleukins (*ILs*) not observed in adult tissues [e.g. *IL-6* transducer, *IL-23* and *IL-33* or their receptors (*IL-F2*)] were also over-expressed. Several transcripts were validated by real-time polymerase chain reaction (QPCR) and immunohistochemistry. QPCR showed that *casp 6* was increased after 1 × KA but reduced after 3 × KA; the pro-inflammatory gene *Cox1* was either upregulated or unchanged after 1 × KA but reduced by ~70% after 3 × KA. Enhanced GFAP immunostaining following 1 × KA was selectively attenuated in the CA1 subregion after 3

Correspondence: Dr Linda K. Friedman, as above. Linda_Friedman@nymc.edu or lfriedma@aol.com.

Supporting Information

Additional supporting information can be found in the online version of this article:

Table S1. Total number of regulated genes after 1 × KA and 3 × KA. Intensity fold-changes (negative for down-regulation) with respect to control animals after one or three injections of KA are illustrated under columns (1K/C) or (3K/C). P-VAL is the *P*-value of the heteroscedastic *t*-test of the equality of the mean expression values in KA (K) vs. control (C) injected animals under 1.5× fold-change and $P < 0.05$ criteria.

Table S2. Total number and description of uncommonly up-regulated genes after 1 × KA and 3 × KA. Intensity fold-change in gene expression with respect to control animals were based on the value of 1K/C or (3K/C) exceeding 2.0 and $P < 0.05$. Each gene is described by symbol and biological process.

× KA. The observed differential transcriptional responses may contribute to early-life seizure-induced pre-conditioning and neuroprotection by reducing glutamate receptor-mediated Ca^{2+} permeability of the hippocampus and redirecting inflammatory and apoptotic pathways. These changes could lead to new genetic therapies for epilepsy.

Keywords

calcium; conditioning; development; hippocampus; microarray; seizures

Introduction

Although seizures are known to be harmful due to excessive release of glutamate and overactivation of glutamate receptors, a large number of recent studies in mature animals have also shown that protective effects can be observed if status epilepticus is preceded by a mild seizure or sublethal ischemia insult. In adult rats or mice, highly sensitive to neuronal cell death, a short episode of kainate (KA)-induced status epilepticus, ischemia, hypoxia, electroconvulsive shock, or audiogenic seizures protects vulnerable neurons from subsequent prolonged insults (Kitagawa *et al.*, 1991; Kutsuwada *et al.*, 1992; Kelly & McIntyre, 1994; Sedlak *et al.*, 1995; Sem'yanov *et al.*, 1997; Najm *et al.*, 1998; Kondratyev *et al.*, 2001; Semenov *et al.*, 2008; Nemethova *et al.*, 2010). The mechanisms underlying preconditioning neuroprotection in mature animals are beginning to be elucidated. Recent studies have illustrated that subthreshold stimuli activate growth and differentiation signals (e.g. ERK and p38 pathways) to protect from ischemic injury (Jiang *et al.*, 2003; Jones & Bergeron, 2004). Glial glutamate transporters also appear to be involved in this type of protection in the mature brain, as several transporter subtypes were upregulated after hypoxic preconditioning (Yu *et al.*, 2008) and loss of glial Glut-1 transporter prevented the neuroprotective effects (Geng *et al.*, 2008). Similarly, pre-treatment with low concentrations of glutamate or *N*-methyl-D-aspartate (NMDA) to mature cultured neurons protects from oxygen–glucose deprivation and/or glutamate-, NMDA- and KA-induced neurotoxicity (Ogita *et al.*, 2003; van Rensburg *et al.*, 2009).

Our recent *in vivo* studies show that a sub-maximal stimulus in early development does not lead to tolerance as in adults. In a normal developing brain, tolerance that leads to self-protective mechanisms is best achieved if the first insults, e.g. on postnatal day (P)6 and P9, are maximal and long-lasting, suggesting that the genetic background and amount of perinatal activity are critical for long-term adaptations that will lessen upcoming seizure severity and lethal damage (Saghyan *et al.*, 2010). Attenuation of Ca^{2+} responses and age-dependent shifts in the ratio of AMPA and NMDA receptor subunits are involved in the early-life seizure response (Friedman, 2006; Friedman *et al.*, 2008; Saghyan *et al.*, 2010). Accordingly, our *in vitro* experiments revealed that high to maximal concentrations of glutamate or NMDA (but not AMPA), were most effective in increasing neuronal survival upon subsequent exposure if introduced early in cultured hippocampal life, and further confirmed that NMDA receptors and calcium-binding proteins were involved in the protection (Friedman & Segal, 2010). Morphological and physiological studies in neonatal and juvenile rats have demonstrated different changes in dendritic arbor and spine density

which depend upon when seizures begin, and that partial pruning and reduced glutamate receptor-mediated Ca^{2+} permeability of the hippocampus may contribute to the subsequent neuroprotection (Jimenez-Mateos *et al.*, 2008; Saghyan *et al.*, 2010).

Microarray transcriptome profiling of the isolated CA1 subregion was applied to identify genes involved in the protective effects caused by multiple early-life perinatal seizures. We compared gene expression profiles of the CA1 from control juvenile animals with juvenile animals with either a single injection of KA (1 × KA) or three such injections (3 × KA). We found a differential transcriptional response in animals with a history of two prior neonatal seizures, such that a number of protective gene candidates may be tested in future studies to determine their role in neuronal fate decisions.

Materials and methods

KA-induced status epilepticus

Lactating female Sprague–Dawley rats with 10 male pups were obtained from Charles River Laboratories, Wilmington, MA, USA. They were first received and maintained under quarantine for 2 weeks at room temperature (55% humidity) in accordance with NIH guidelines and approval by our Institutional Animal Care and Use animal Committee (IACUC) at New York College of Osteopathic Medicine. Rats were given food and water *ad libitum* on a 12-h light–dark cycle and the healthy male litters were kept with their lactating mother for the duration of the experiments. To induce seizures, we used our previously established protocol of multiple early-life seizures with KA (Ascent Scientific, Princeton, NJ, USA) as described (Liu *et al.*, 2006). Neonate (P6 and P9) and juvenile (P20) rats were injected with 1 × KA (on P20, 9–10 mg/mg i.p.) or 3 × KA (P20, 9–10 mg/mg i.p.; P6 and P9, 2 mg/kg s.c.; $n = 8$ per condition) and killed 72 h after the last harmful seizure. Equal numbers of age-matched control littermates ($n = 8$) were injected with equivalent volumes of phosphate-buffered saline (PBS; 0.1 M, pH7.4). After KA injection, rats were placed in a clean and comfortable cage and their epileptic behavior was continuously monitored and scored every 5 min for 2 h. At the younger age groups, P6 and P9, seizure severity ratings were similar for all animals used in the study. P6 and P9 pups with 1 × KA or 3 × KA were scored according to their behaviors on a scale of 1–4, with side tonus rated as the highest score and scratching as the lowest. To meet the criteria for later tissue isolation, presentation of a specific behavior, loss of postural control and long bouts of lying on one side in a tonic position (side tonus), for at least 1.5 h, was required (Liu *et al.*, 2003; Liu *et al.*, 2006). For the older age group (P20), seizure rating was determined using the Racine method on a scale of 0–7 with 0 representing normal behavior and 7 representing death (Liu *et al.*, 2006). Rated scores were averaged and subjected to statistical analysis. Only rats that exhibited one or three episodes of status epilepticus were used in this study.

Hippocampal microdissection

After decapitation, the entire brain was quickly removed under RNAse-free conditions from age-matched control and experimental rats then placed into ice-cold (4 °C) saline and quickly transferred to Mg^{2+}-free artificial cerebrospinal fluid (ACSF) solution equilibrated with 95% O_2 and 5% CO_2. The composition of ACSF was (in mM): NaCl, 130; KCl, 3;

NaH_2PO_4, 1.25; $NaHCO_3$, 26; glucose, 10; and $CaCl_2$, 3 (pH 7.3–7.4). Under a dissection microscope, the CA1 was bilaterally dissected away from the CA3 and DG subregions with iridectomy scissors on an ice platform. Three cuts were made to separate the subfields. The DG, also including some of the hilus, was carefully removed. The CA3 was then removed, followed by the CA1 which also included the subicular area. The white matter overlying the CA1 and CA3 was also dissected away. Dissected tissue fragments from each area were quickly transferred to Eppendorf tubes and kept on dry ice until all dissections were complete. Samples were stored at −80 °C until use. Total RNA was isolated from the CA1 subregion of the hippocampus from the three groups and processed for the microarray experiments.

Microarray analysis

The present study used the protocol optimised in our laboratory (Adesse *et al.*, 2010) in accordance to the standards of the Microarray Gene Expression Data Society. Briefly, 30 lg of total RNA was extracted in TRIzol (Invitrogen Corporation, Carlsbad, CA, USA). Four biological replicas were generated from CA1 tissue fragments that were pooled into one microcentrifuge Eppendorf tube from two animals for each group. Thus, a total of four samples per condition were generated and each sample contained tissues from two animals, yielding a total of eight animals per group (n = 24 rats). Extracted RNA was then reverse-transcribed in the presence of fluorescent Alexa Fluor® 555-aha-dUTP (green fluorescent emission) or Alexa® 647-aha-dUTP (red emission; Invitrogen) to obtain a green- or red-labeled cDNA sample. This procedure was repeated for each condition with new arrays, yielding four biological replicas per group. Differently labeled RNA samples were co-hybridised (‘multiple yellow’ strategy; Iacobas & Iacobas, 2011) overnight at 50 °C with rat 27k oligonucleotide arrays printed by Duke University (full technical information in http://www.ncbi.nlm.nih.gov/geo/query/acc.cgi?acc=GPL9207). Thus, control (saline treated) was hybridised against the control in two arrays and experimental (1 × KA or 3 × KA) against experimental in two other arrays, green experimental being compared to green control, red experimental to red control, green and red ratios being averaged. The multiple-yellow strategy uses 100% of the resources (dye-swapping and reference samples are no longer necessary with this advanced method). Moreover, this procedure has maximum flexibility (four biological replicas being hybridised) to provide the best normalisation (Iacobas *et al.*, 2008). After hybridisation, the slides were washed at room temperature with solutions containing 0.1% SDS and 1% SSC (3 M NaCl + 0.3 M sodium citrate) to remove the non-hybridised cDNAs. All spots affected by local corruption, or with saturated pixels, or with foreground fluorescence less than twice the background fluorescence, were removed from the analysis. The background-subtracted signals were normalised iteratively, alternating red/green, inter-block, lowest and scale intra-slide and inter-slide normalisation until the fluctuation of the ratio between the spot median and the corresponding block median of valid spots became < 5% between successive iteration steps (Spray & Iacobas, 2007). Normalised expression levels were organised into redundancy groups (each group composed of all spots probing the same gene) and represented by the weighted average of the values of individual spots. A gene was considered as significantly regulated under two criteria: (i) if the absolute fold-change was > 1.5 × or (ii) ≥ 2v and the P-value of the heteroscedastic t-test applied to the means of the background-subtracted normalised fluorescence values in the

four biological replicas of the compared transcriptomes was < 0.05. In addition, absolute fold-changes were also filtered at ≥ 3.0 × and ≥ 4.0 × order to separate gene categories most affected by in status epilepticus. This composite criterion in which the *P*-values (two-samples, unequal variance) were computed with Bonferroni-type corrections applied to the redundancy groups eliminates a great number of false hits without increasing significantly the number of false negatives (Iacobas *et al.*, 2005). We have previously validated our method (Soares *et al.*, 2010).

Gene categories

GenMapp and MappFinder programs (www.genmapp.org; Gladstone Institute, University of California at San Francisco, USA) were used to determine whether altered gene expressions differed significantly from chance for the overlapping functional and structural gene ontology categories.

Quantitative PCR (QPCR) analysis

The effects of one or multiple induced seizures on the expression of genes related to NMDA receptor (NMDAR) function, apoptosis and related signaling pathways were assessed from the CA1 via standard QPCR methodology (n = 7 per group). The following genes were selected: NR2A (GRIN2A subunit of the NMDAR), NR2B (GRIN2B subunit of the NMDAR), Casp3 (caspase 3), Casp6 (caspase 6), Calm2 (calmodulin 2) and Cox1 (cyclooxygenase 1). Rat hippocampal CA1 material (~3–5 mg) obtained from bilateral hippocampal microdissection (see above) was homogenised on wet ice with pestle and mortar. Total RNA was prepared from each tissue using the RNeasy RNA-isolation system in combination with QIA shredder columns according to the manufacturer's specifications (Qiagen, Valencia, CA, USA). RNA concentration and integrity were determined via standard spectrophotometry and agarose gel-electrophoresis. Reverse transcription RT-PCR was performed using the Superscript III First-Strand Synthesis System for RT-PCR (Invitrogen). QPCR was carried out using Power SYBR Green PCR Master Mix (Applied Biosystems, Foster City, CA, USA) with rat β-actin as a relative standard. DNA primers were designed using the Integrated DNA Technologies Primer Quest tool (IDT, Coralville, IA, USA). The following gene-specific DNA primers were used for all experimental groups: β-actin forward, 5′- TGA GAG GGA AAT CGT GCG TGA CAT -3′; β-actin reverse, 5′- ACC GCT CAT TGC CGA TAG TGA TGA -3′; Calm2 forward, 5′- CAA CTG ACT GAA GAG CAG ATC GCA -3′; Calm2 reverse, 5′- TGC CAT TAC CGT CGG CAT CTA CTT -3′; Casp3 forward, 5′- TGG AGA AAT TCA AGG GAC GGG TCA -3′; Casp3 reverse, 5′- TCC GGT TAA CAC GAG TGA GGA TGT -3′; Casp6 forward, 5′- TTT AAC GAC CTC CGG GCA GAA GAA -3′; Casp6 reverse, 5′- ATG CGT AAA TGT GGT TGC CTT CCC -3′; Cox1 forward, 5′- ATT GGA GGC TTC GGG AAC TGA CTT -3′; Cox1 reverse, 5′- ACT GTT CAT CCT GTT CCA GCT CCA -3′; NR2A forward, 5′- ATC ATG GCT GAC AAG GAT CCG ACA -3′; NR2A reverse, 5′- TTC AGC ATA ACT GTG GCT TGC TGC -3′; NR2B forward, 5′- ATG GTA TCT CGC AGC AAT GGG ACT -3′; NR2B reverse, 5′- ACC GCA GAA ACA ATG AGC AGC ATC -3′.

Immunohistochemistry

Immunohistochemistry with the astrocytic marker glial fibrillary acidic protein (GFAP) was performed in fresh free-floating coronal vibratome sections (40 μm) derived from control and experimental animals from all groups at the level of the hippocampus. Rats were anesthetised with a lethal dose of sodium pentobarbital (25 mg/kg) and quickly perfused intra-aortically with 50 mL of ice-cold 0.9% saline followed by 200 mL of 4% PFA in 0.1 M PBS. Cut sections were first submerged in quenching solution (0.1% H_2O_2 in PBS) for 30 min, rinsed four times with PBS, and then incubated in 1% BSA and 0.2% Triton X-100 for 30 min. GFAP (Sigma) was used to visualise changes in acute proliferating astrocytes as well as changes in astrocytic morphology. Sections were incubated with the GFAP antibody dilution (1: 1000 in 0.5% BSA) overnight at 4 °C. A biotinylated rabbit antibody was used as a secondary antibody. Sections were rinsed three times in PBS and placed in ABC solution (Vector Laboratories) for 1 h. Reaction products were detected using with 3′, 3-diaminobenzidine tetrahydrochloride for visualisation as above. Immunohistochemical studies were performed in controls rats, after 1 × KA and after 3 × KA, at 72 h following the last KA injection ($n = 4$, $n = 5$ and $n = 6$, respectively). After mounting sections on slides, dehydration in graded ethanols, clearing and coverslipping, hippocampal sections were scanned with a digital spot camera attached to an Olympus BX51 microscope interfaced with a Pentium IV DELL computer. All camera settings were held constant during image capturing.

Cell counting

To estimate the volume fraction of astrocytes of the CA1 subregion after 1 × KA vs. 3 × KA, counting of GFAP-stained astrocytes was carried out within a defined area of four consecutive 0.7-mm^2 sectors in the middle of the CA1, similar to procedures described by Wang *et al.* (2004). A grid reticule (100 μm × 0.10 mm), inserted into the eyepiece, with a 20 × objective was aligned along the CA1 from both hemispheres, and a manual cell counter was used by a senior faculty member blind to the experimental conditions. To avoid overlap, sections were first randomised from four hippocampal levels [every 5th and 15th section between −2.4 and −4.6 mm from bregma (Paxinos *et al*., 1980)]. In addition, cells were− also counted manually with assistance from Pro Image software, from four sections at three levels per animal after scanning them into an Olympus BX51 microscope interfaced with a Pentium IV DELL computer. Counts from the two counting methods were averaged into a grand mean per group. Percentages of GFAP-labeled cells were then calculated for each area relative to respective controls.

Statistics

Significant differences were determined for microarray intensity differences as described above. Numbers assessed from counting of GFAP-stained glia were averaged from at least four sections from four levels of the dorsal hippocampus per animal, then subjected to one-way factorial analysis (ANOVA). QPCR averages were analysed by repeated-measures ANOVA as appropriate using GB-Stat software (General Dynamics, Bethesda, MD, USA) for Macintosh. Data are reported as mean ± SEM. The probability level interpreted as significant was $P < 0.05$ for all tests.

Results

Microarray profile of hippocampal CA1 affected by single vs. multiple early-life seizures

Data complying with the Minimum Information About Microarray Experiments (MIAME) were deposited in the NCBI database (http://www.ncbi.nlm.nih.gov/geo) as series GSE44031 (Table S1). In this experiment, 9834 genes were adequately quantified under all three conditions. Total regulated gene pathways were quantified under several criteria (see Materials and Methods). To determine which genes were significantly altered, filtering was carried out at 1.5×, 2×, 3× and 4× absolute fold-change.

Under the 1.5× and $P < 0.05$ criterion, many more genes were regulated following 3 × KA (9.6%) than following 1 × KA (7.1%; Fig. 1A). Scatter plots of mean signal intensities of each transcript were plotted against their $\log_{10}$ expression ratio (1 × KA vs. Control, 3 × KA vs. Control, 3 × KA vs. 1 × KA), showing normal distributions of regulated genes with high correlation coefficients (≥ 0.97; Fig. 1A). After 1 × KA there were few downregulated genes (41) and many upregulated genes (670). After 3 × KA, fewer genes were downregulated but more genes were upregulated (910; Fig. 1B). Only 11 genes were commonly downregulated (Table 1).

Under the 2× criterion, 426 genes were significantly upregulated and 18 genes were significantly downregulated after 1 × KA. After 3 × KA, 599 genes were significantly upregulated and 20 genes were significantly downregulated (Fig. 1C). This criterion revealed only five commonly downregulated gene transcripts (indicated with ** in Table 1) and 243 commonly upregulated genes (found in Table S1). When comparing 3 × KA vs. 1 × KA, the number of significantly differentially downregulated genes increased and the total number of significantly differentially upregulated genes decreased, due to a large percentage of commonly upregulated genes (Fig. 1B and C).

Under the 3.0× criterion, 96 genes were significantly upregulated and only three genes were significantly downregulated (*Cox7b*, *Ints10* and *S100a5*) after 1 × KA. After 3 × KA, 123 genes were upregulated and eight genes were downregulated.

Under the 4.0× criterion none were downregulated in either group but 25 genes and 29 genes were increased with respect to control following 1 × KA and 3 × KA, respectively. After calculating the ratio of the experimental groups (3 × KA: 1 × KA), the slope of plotted transcripts became even closer to 1 ($m = 0.969$), suggesting that only a unique set of genes were differentially regulated by the two different treatment paradigms at the time examined, consistent with adult studies (Borges *et al.*, 2007).

Ontologies for genes regulated after 1 × KA vs. 3 × KA

GenMapp and gene ontology software were used to identify global biological trends in gene regulation, similar to that described in adult models of epilepsy (Gorter *et al.*, 2006; Jimenez-Mateos *et al.*, 2008). Significance was represented by a Z-score [Figs 2-4; grey line for genes that were over-represented (≥ 2) or under-represented (≤ −2)]. The ontology of genes regulated is graphically plotted as 1 × KA vs. control, 3 × KA vs. control, and 3 × KA vs. 1 × KA.

Within the category of biological process, the largest changes in gene expression after 1 × KA were under cellular process, metabolism, biological process, developmental process, localisation, multicellular organisational process, and response to stimulus, and genes were predominantly upregulated (Fig. 2A, D and G). After 3 × KA, the largest number of genes regulated was in the same categories as the animals treated with 1 × KA; however, more genes were over-expressed (Fig. 2B, E and H). In addition, genes within multicellular organisational process were over-represented. When comparing the ratio 3 × KA: 1 × KA; the number of genes differentially expressed increased (Fig. 2C, F and I). The number of differentially downregulated genes also increased (comparing the ratio of the two groups; Fig. 2I).

Within the category of cellular component, the largest numbers of genes regulated were associated with cell part, organelle and organelle part after both 1 × KA and 3 × KA (Fig. 3). Additional differentially downregulated genes were observed when comparing the ratio (Fig. 3C, F and I).

Within the category of molecular function, the largest number of genes regulated was associated with binding, catalysis, molecular transducer, transcription regulator and transporter after 1 × KA and after 3 × KA (Fig. 4A–I). Additional differentially downregulated genes were also revealed when comparing the ratio which fell under molecular transducer under molecular; and more upregulated genes were found under translation regulator (Fig. 4G–I). Z-scores are presented for each category.

Commonly regulated gene pathways

The five genes that were commonly downregulated under the 2× criterion fell under different biological functional categories, such as growth and survival signaling, ion transport, membrane stability and calcium binding (Table 1). Some examples of commonly upregulated genes following 1 × KA or 3 × KA include glutamatergic kainite 1 (*Grik1*), the caspase activation inhibitor *Aven* and the Ca^{2+} channel voltage-dependent γ4 subunit.

Certain pro-inflammatory genes that were commonly upregulated after either single or multiple episodes of status epilepticus include GFAP (> 6.0), the major astrocytic marker, and vimentin (*Vim 2.4* and *2.7*, respectively). Additionally, fibroblast growth factors, tumor necrosis factor receptor and *Hdac1*, a histone deacetylase that may be involved in regulating the expression of pro-inflammatory interleukin 10, were commonly upregulated. Anti-inflammatory interleukin genes that regulate different protective responses of the immune system and that were commonly upregulated were *IL-13* and *IL-23* (see Table S1).

Uniquely downregulated genes

There were only 13 and 15 uncommonly downregulated genes after 1 × KA and 3 × KA, respectively; some of these may lead to neuroprotective differences in response to the seizure insult(s) (Fig. 1C and Tables 2 and 3). For example, a uniquely downregulated gene after 1 × KA when injury occurs was *Calm2*, serving in an important Ca^{2+}-signaling pathway for cell survival decisions. Loss of additional genes encoding proteins that regulate Ca^{2+} homeostasis, oxidative phosphorylation, inflammation, respiration and neurogenesis

were also observed following the first seizure at P20; these include *Cox7b* and *S100A5*, which may facilitate neuronal cell death. In contrast, an example of a uniquely downregulated gene after 3 × KA, one that may contribute to tolerance, was loss of *Atp11a*, the integral membrane ATPase which would reduce the transport of calcium ions across cell membranes and inhibit downstream neurotoxic events (Table 3). Additional differentially downregulated genes include *Itpka* and *Casp6*, which are involved in inositol phosphate metabolism and apoptotic signaling pathway decisions. *Kcnh6* and *Sstr5* were also decreased; these contribute to neuronal excitability and adrenocorticotropin secretion, respectively (Fig. 1A and Supporting Information Table S1). After calculating the ratio of intensities of 3 × KA: 1 × KA, *calm2* was found to be increased and this may contribute to neuronal survival after multiple early-life seizures.

Uniquely upregulated genes

There were 183 uniquely upregulated genes expressed after 1 × KA, whereas 356 gene transcripts were increased after 3 × KA (Fig. 1C; Table S2). Examples after 1 × KA include *S100a4, Nadsyn1, Kcng1, Aven* and *Hrsp12*, genes involved with neurotransmitter release, calcium binding, excitability, inflammation and metabolic redox reactions (Fig. 1A). Heat-shock transcription factor 4 (*Hsf4*), involved in inflammation, exhibited opposite signaling in that it was increased after 1 × KA (2.4) but decreased after 3 × KA (−1.7). Examples of genes uniquely upregulated after 3 × KA and that favor neuroprotection include peroxide- and GABA-synthesising enzymes such as *Cat, Gpx7* and *Gad1*. Additional upregulated genes that service neuroprotection after 3 × KA include *GRP1* (general receptor for phosphoinositides 1-associated scaffold protein; *Grasp*), which plays a role in intracellular trafficking and contributes to the macromolecular organisation of group 1 metabotropic glutamate receptors (Table S2).

Genes encoding anti-stress heat shock protein (*Hspa12A), Foxn1*, adenosine A1 receptor and Ca^{2+} adaptor and homeostasis proteins such as *Cacnb4 and Atp2b2* were also uniquely increased. Other examples of genes that can lead to neuroprotection include *Bcl-2* gene members, intracellular trafficking protein and *Grasp*, as well as *Foxn1, Gad1, Bnip2* and *Bag4*, which are involved with immunity, with excitatory and inhibitory neurotransmission and with anti-apoptotic processes (Fig. 1A and Table S2). After calculating the ratio of intensities of 3 × KA: 1 × KA, *Inpp1* also appeared differentially upregulated; it is involved in phosphatidylinositol signaling pathways. Further, differentially upregulated interleukins observed only after 3 × KA possess anti-inflammatory abilities [(e.g. *IL-6* transducer, IL-F2 and suppressor of cytokine signaling (*Socs3*)]. In adult study findings, commonly increased genes include pro-inflammatory interleukins of the *IL-1* or *IL-5* to *IL-12* family; however, such family members were not altered at the time point examined in our study. Additional protective genes that were upregulated after 3 × KA, but unaltered after 1 × KA, include adaptor proteins such as the adaptor protein complex *AP-1, sigma 1*, adaptor protein phosphotyrosine interaction, and adaptor-related protein complex 3 μ2 subunits.

Uncommonly regulated gene pathways

General ion pathways with differential regulation were in Ca^{2+}, Zn^{2+} and Mn^{2+} binding as well as K^{+} ion transport. The pathway that that had the most differentially regulated genes

(uniquely upregulated) was in Ca^{2+} signaling (Table S2). Several annexins and S100 proteins representing two large, but distinct, Ca^{2+}-binding protein families were differentially regulated; annexin 3 and cadhedrin 15 were increased after 3 × KA but not after 1 × KA (Table S2). In addition, Ca^{2+} channel, voltage-dependent gamma subunit 1 (*Cacng1*) and Ca^{2+}-dependent secretion activator, which may increase Ca^{2+} transport, were significantly increased only after 3 × KA. Certain Na^{+} channels were also differentially expressed (Table S2). The second main pathway that showed large differential changes in gene expression was in cytoplasmic vesicle and membrane-bound vesicle. These involved the Golgi membrane and coated vesicles, particularly within the GABA receptor family.

Another critical pathway differentially altered was under apoptosis. Examples of protective genes differentially upregulated after 3 × KA were anti-apoptotic *Bcl-2* gene members including the *Bcl-2-modifying factor* (*Bmf*), *Bcl-2/adenovirus E1B interacting protein 2* (*Bnip2*), *Bcl6-interacting co-repressor* (*Bcor*) and *Bcl-2-associated athanogene 4* (*Bag4*), which can prevent caspase activation and support neuronal survival. After calculating the ratio, Casp6, an apoptosis executor, was also differentially downregulated and an apoptosis-associated speck-like protein containing a C-terminal caspase-recruitment domain (*Pycard*) was increased only after 1 × KA (Table S1 and Figure 3). Finally, additional pathways with significant differential regulation after 3 × KA vs. 1 × KA fell under negative regulation of transcription and developmental processes such as the notch signaling pathway, Wnt receptor signaling pathway, embryonic development, striated muscle development, mesoderm morphogenesis, chordate embryonic development, forebrain development, and pattern-specific processes.

QPCR validation

For verification of our microarray results, a transcriptional analysis of six genes (*NR2A, NR2B, Casp6, Casp3, Cox1* and *Calm2*) via QPCR was carried out on RNA derived from CA1 hippocampal tissue from separate groups of animals: Controls, 1 × KA and 3 × KA ($n = 7$). Despite a downward trend for *NR2A, NR2B, Casp3* and *Calm2* and an upward trend for *Casp6 and Cox1*, one episode of induced status epilepticus did not produce any statistically significant changes in the expression of the selected genes (Fig. 5A–F). However, the notable increase in *Casp6* expression after 1 × KA and decrease after 3 × KA is consistent with our microarray findings. Following 3 × KA, both NR2A and NR2B genes were significantly reduced, by 50 ± 20% and 70 ± 10%, respectively (Figure 5A and B). In keeping with this general trend, expression of *Casp3* and *Casp6*, which are involved in the execution of cell apoptosis, were significantly reduced by 70 ± 10 and 50 ± 10%, respectively (Figure 5C and D). Furthermore, expression of the calcium modulator gene *Calm2* and the pro-inflammatory gene *Cox1*, which are both involved in apoptotic cell fate decisions, was significantly reduced after 3 × KA by 72 ≥ 10 and 70 ± 10%, respectively (Figure 5E and F).

Inflammation biomarker of gene regulation

The astrocytic marker GFAP has been previously reported to increase after status epilepticus (Represa *et al.*, 1993; Laurén *et al.*, 2010) due to delayed gliosis. GFAP RNA levels were raised by over six-fold after 1 × KA; therefore, immunohistochemistry was used to validate

the microarray experiment. Similar to gene expression results, GFAP protein was enhanced after single and multiple KA seizures but with distinct patterns of expression that included morphological alterations of astrocytes that differed between the two seizure groups (Figure 6). In controls, astrocytes were typically star-like in appearance, exhibiting thin fibers; staining was light and uniform across the hippocampal subfields with the highest density being outside the principle cell layers in structures such as the hilus, stratum radiatum and stratum lacunosum moleculare (Figure 6A–C). After 1 × KA, there was an increase in GFAP staining intensity and the number increased within the CA1 area. Astrocytes were also changed in appearance. They were very dark with thick stubby projections, particularly notable in the lacunosum moleculare (Figure 6D–F). In contrast, after 3 × KA, astrocytic labeling and number of astrocytes appeared similar to controls in the CA1 subregion. Interestingly, staining intensity and morphology resembled that of KA-treated animals within other sublayers, particularly within the hilus and lacunosum moleculare, regions rich in synapses (Figure 6G–I). Quantifying the number of astrocytes confirmed that significant increases in astrocyte proliferation (approximately two-fold) were restricted to the vulnerable CA1 subregion at the 72-h time point examined (Figure 6J).

Discussion

In the juvenile period, we previously showed that two early neonatal seizures on P6 and P9 may serve as a preconditioning stimulus by reducing NMDA responses and injury of the CA1 subregion in P20 rats subjected to a third seizure (Liu *et al.*, 2006; Friedman *et al.*, 2007; Saghyan *et al.*, 2010). This study is the first report to examine transcriptomic profiling of the immature hippocampal CA1 with prior early-life seizure preconditioning. The time-point examined after KA-induced status epilepticus was selected to coincide with the period when histological injury is evident (Liu *et al.*, 2006); this also corresponds to young juvenile ages in children (Haut *et al.*, 2004). The transcriptome profile after 3 × KA differed significantly from the profile generated by a single seizure induced on P20 (1 × KA), suggesting that a unique set of genes may be responsible for the protective effects of the earlier neonatal conditioning seizures.

Microarray gene profiling in adult models of epilepsy

Microarray profliling studies of the mature hippocampus following sustained seizures that cause the progression of epilepsy have also identified robust but somewhat different gene expression changes observed at young ages (Gorter *et al.*, 2006; Hatazaki *et al.*, 2007; Green *et al.*, 2009). Biological pathways identified in the adult hippocampus were predominantly in oxidative stress, gliosis, inflamation, potassium kinetics, and glutamatergic and GABAergic ionotropic neurotransmission. After epileptic preconditioning in mature animals, functional studies showed neuroprotection was associated with attenuated Ca^{2+} responses and fewer spontaneous seizures (Jimenez-Mateos *et al.*, 2008). In addition, certain protective genes such as the anti-apoptotic gene regulator *Mapk8ip* increased while other toxic genes were simultaneously downregulated in vulnerable neurons (Jones & Bergeron, 2004; Hatazaki *et al.*, 2007). At 24 h prior to significant cell death, another microarray study showed that the largest changes in gene expression were in the dentate gyrus, a region resistant to cell death, suggesting that both upregulation of neuroprotective phenotypes and

downregulation of toxic transcripts within specific hippocampal subregions may be required to obtain full epileptic tolerance in mature animals (Arundine & Tymianski, 2004; Borges *et al.*, 2007).

Molecular studies in juvenile models of epilepsy and protective signaling pathways

In contrast to observations in adult seizure models, the main biological pathways affected after a single episode or after multiple episodes of KA-induced status epilepticus in the developing brain were in categories of calcium and zinc binding, negative regulation of transcription and in growth and developmental processes such as the Notch and Wnt signaling pathways. Furthermore, multiple early-life seizures may lead to enhanced GABA sythesis and subsequent epiletptic tolerance and neuroprotection, as *Gad1* (glutamic acid decarboxylase 1) was differentially increased after 3 × KA, suggesting that an increase in inhibitory neurotransmission occurs with increased number of early-life seizures. Our original age-dependent observations in gene and protein expression of glutamatergic and GABAergic systems as a result of status epilepticus suggested tolerance could be developed if seizures began early during postnatal development (Friedman, 2006). Accordingly, QPCR showed reduced NMDAR2 receptor subunit expression after multiple seizures; this is consistent with our previous immunohistochemistry report that showed reduced protein expression and NMDA receptor activation in the CA1 (Saghyan *et al.*, 2010).

Consistent with other reports (Jimenez-Mateos *et al.*, 2008), differential gene regulation was particularly apparent for many Ca^{2+}-binding genes. The endoplasmic reticulum (ER), a major source of $[Ca^{2+}]_i$ uptake, was regulated. For example, inositol triphosphate (IP3) receptor members of a family of Ca^{2+} channels that control Ca^{2+} release from the ER into the cytosol to trigger many cell functions including excitability, transmitter release, synaptic plasticity, gene expression and neurotoxicity were differentially activated (Simpson *et al.*, 1995). The intracellular phospholipase-C (PLC) signaling pathway was triggered after 3 × KA, and QPCR showed that *Calm2* decreased with increasing seizures. This suggests that other mobile Ca^{2+} buffers, such as the calbindins, paravalbumin, and S100 protein families that blunt Ca^{2+} spiking, were affected and potentially assist in redistribution of Ca^{2+} ions into survival signaling pathways. This is also consistent with a recent microarray study of the isolated CA1 subregion during the juvenile period (at P21) 1 week following a single episode of KA-induced status epilepticus (Laurén *et al.*, 2010). In view of this, inhibition of Ca^{2+} release with dantroline via ryanodine receptors after status epileptcus is neuroprotective (Popescu *et al.*, 2002).

The other pathway that generates IP3, and that is initiated by phosphoinositide 3-kinase (PI3K), includes an enzyme that phosphorylates inositol lipids to produce two signaling molecules, PIP2 (phosphatidylinositol 3,4-bisphosphate) and PIP3 (phosphatidylinositol 3,4,5-trisphosphate) and can induce cell death (Xu *et al.*, 2005). IP3, generated from PIP2, influences cell division, cell proliferation, apoptosis, fertilisation, development, behavior, memory and learning processes, consistent with gene ontology terms altered in our CA1 microarray study. We also found that *Ip3kB* was upregulated in the CA1 of both 1 × KA- and 3 × KA-treated animals whereas *Ip3kC* was increased only after 1 × KA, suggesting that reducing the latter enzyme would suppress intracellular Ca^{2+} overload from the ER to afford

protection. Accordingly, *Bcl-2* overexpression and reduced subsarcolemmal and mitochondrial Ca^{2+} overload in myotubes during activation of nicotinic acetylcholine receptors produced protection and contributed to inhibition of IP3Rs (Basset *et al.*, 2006). Moreover, annexins and S100 proteins were differentially regulated, and this is also consistent with a recent clinical report (Choi *et al.*, 2009). Collective changes may contribute to the reduced Ca^{2+} responses after multiple seizures observed in our Ca^{2+} imaging study following multiple early-life seizures (Saghyan *et al.*, 2010).

Inflammation

It is well known that Induction of inflammatory mediators following an insult is age-dependent. In adults, GFAP, *IL-1*, tumor necrosis factor (TNRα) and *IL-6* increase in response to injury or models of inflammation (Layé *et al.*, 1994; Vallières & Rivest, 1997; Yang *et al.*, 2009), whereas in neonates GFAP is unchanged and *IL-1b, IL-6, IL-23* and *IL-10* are acutely increased (within 24 h post-LPS treatment; Ortega *et al.*, 2011). GFAP increases observed herein after single or multiple seizures were similar to those in other reports (Yang *et al.*, 2009; Laurén *et al.*, 2010). However, our immunohistochemical study also revealed that the enhanced GFAP staining and changes in morphology that occur after 1 × KA were selectively attenuated in the CA1 subregion after 3 × KA, suggesting that signaling pathways regulating inflammation are differentially affected among different anatomical regions and may contribute to the neuroprotection. Distinct interleukins, not observed in adult tissues, such as anti-inflammatory cytokines (*IL-S6* transducer, *IL-23* and *IL-33*) or their receptors (ILF-2) that support neuronal survival, were over-expressed after 3 × KA. This was not surprising, as the immune system of infants is distinguishable from that of adults and is consistent with the types of interleukins that are detected in human neonatal cord blood (Hebra *et al.*, 2001). Although *IL-6* encodes genes with pro-inflammatory properties, it also has anti-inflammatory properties that are reported to coincide with induction of *Bcl-2* anti-apoptotic members, but not superoxide dismutase activation, consistent with our array of gene expression (Ward *et al.*, 2000). Increases in *IL-6* have been observed after hypothermia, ischemia and LPS injection and these increases may contribute to cell death or could contribute to pre-conditioning and subsequent tolerance involving the Toll receptor pathway (Vallières & Rivest, 1997; Feng *et al.*, 2007; Stewart *et al.*, 2010; Fan *et al.*, 2011). In addition, it has been demonstrated that LPS can induce ceramide upregulation in brain cortex; LPS is a downstream messenger in TNF-alpha signaling which may contribute to hypoxia-induced tolerance in neuronal cells (Zimmermann *et al.*, 2001). Thus, differential regulation of several cytokines and their receptors may contribute to the neuroprotective effect produced by the two earlier conditioning neonatal seizures.

Cell death signaling pathways

Cell death is controlled by caspases that cleave their substrates at specific aspartate residues (Cohen, 1997; Fuentes-Prior & Salvesen, 2004). *Casp3, Casp6* and *Casp7* are ‘effector’ caspases that are activated by death-inducing signaling pathways triggered by *Casp8* or *Casp9* while *Casp6* is central in determining cell fate as it cleaves *casp8* and *casp10* to trigger cell death (Danial & Korsmeyer, 2004; Inoue *et al.*, 2009). Accordingly, differential reduction in *casp6* after 3 × KA was observed in the microarray, and QPCR revealed that the single episode of status epilepticus resulted in a trend for *casp3* to go down and *Casp6* to go

up. This could prevent cell injury and cell death due to lack of subsequent *Casp8* and *Casp10* activations required for cell death. The array also showed that an apoptosis caspase inhibitor (*Aven*) was commonly increased, indicating that tolerance factors arise after the first insult. Several anti-apoptotic Bcl-2 gene members that may inhibit caspase activation to increase neuronal survival were also increased, but only after 3 × KA. In keeping with this, *Bcl-2* was reduced and *Bax* immunoreactivity was sustained in CA1 neurons destined to die following forebrain ischemia which was attenuated with preconditioning (Hara *et al.*, 1996; Nemethova *et al.*, 2010). Similarly, after traumatic brain injury *bcl-2* and *bcl-xL* mRNAs were depressed for days in the hippocampus ipsilateral to injury (Strauss *et al.*, 2004). Likewise, programmed cell death and apoptotic neurodegeneration were attenuated in transgenic mice overexpressing Bcl-2 (Martinou *et al.*, 1994; Cunningham *et al.*, 2004; Cox & Hampton, 2007; Hansen *et al.*, 2007).

In conclusion, three episodes of status epileptcus during the neonatal period caused differential gene regulation to induce specific genes that favor survival signaling pathways. Future directions will be to test candidate genes to reveal their role in cell death and survival decisions during critical periods of development.

Supplementary Material

Refer to Web version on PubMed Central for supplementary material.

Acknowledgements

The present study was supported by New York College of Osteopathic Medicine in-house funding (to LKF) and NIH NS041282 (to DS).

Abbreviations

1 × KA	single injection of KA
GFAP	glial fibrillary acidic protein
IL	interleukin
KA	kainic acid
NMDA	*N*-methyl-D-aspartate
NMDAR	NMDA receptor
P	postnatal day
PBS	phosphate-buffered saline
QPCR	quantitative PCR
3 × KA	three injections of KA

References

Adesse D, Iacobas DA, Iacobas S, Garzoni LR, Nazareth Meirelles M, Tanowitz HB, Spray DC. Transcriptomic signatures of alterations in a myoblast cell line infected with four strains of *Trypanosoma cruzi*. Am. J. Trop. Med. Hyg. 2010; 82:846–854. [PubMed: 20439965]

Arundine M, Tymianski M. Molecular mechanisms of glutamate-dependent neurodegeneration in ischemia and traumatic brain injury. Cell. Mol. Life Sci. 2004; 61:657–668. [PubMed: 15052409]

Basset O, Boittin FX, Cognard C, Constantin B, Ruegg UT. Bcl-2 overexpression prevents calcium overload and subsequent apoptosis in dystrophic myotubes. Biochem. J. 2006; 395:267–276. [PubMed: 16393138]

Borges K, Shaw R, Dingledine R. Gene expression changes after seizure preconditioning in the three major hippocampal cell layers. Neurobiol. Dis. 2007; 26:66–77. [PubMed: 17239605]

Choi J, Nordli DR Jr. Alden TD, DiPatri A Jr. Laux L, Kelley K, Rosenow J, Schuele SU, Rajaram V, Koh S. Cellular injury and neuroinflammation in children with chronic intractable epilepsy. *J. Neuroinflamm.*. 2009; 6:38–52.

Cohen GM. Caspases: the executioners of apoptosis. Biochem. J. 1997; 326(Pt 1):1–16. [PubMed: 9337844]

Cox AG, Hampton MB. Bcl-2 over-expression promotes genomic instability by inhibiting apoptosis of cells exposed to hydrogen peroxide. Carcinogenesis. 2007; 10:2166–2171. [PubMed: 17434928]

Cunningham LL, Matsui JI, Warchol ME, Rubel EW. Over-expression of Bcl-2 prevents neomycin-induced hair cell death and caspase-9 activation in the adult mouse utricle in vitro. J. Neurobiol. 2004; 60:89–100. [PubMed: 15188275]

Danial NN, Korsmeyer SJ. Cell death: critical control points. Cell. 2004; 116:205–219. [PubMed: 14744432]

Fan LW, Tien LT, Lin RC, Simpson KL, Rhodes PG, Cai Z. Neonatal exposure to lipopolysaccharide enhances vulnerability of nigrostriatal dopaminergic neurons to rotenone neurotoxicity in later life. Neurobiol. Dis. 2011; 44:304–316. [PubMed: 21798348]

Feng Z, Davis DP, Sásik R, Patel HH, Drummond JC, Patel PM. Pathway and gene ontology based analysis of gene expression in a rat model of cerebral ischemic tolerance. Brain Res. 2007; 1177:103–123. [PubMed: 17916339]

Friedman LK. Calcium: a role for neuroprotection and sustained adaptation. Mol. Interv. 2006; 6:315–329. [PubMed: 17200459]

Friedman LK, Segal M. Early exposure of cultured hippocampal neurons to excitatory amino acids protects from later excitotoxicity. Int. J. Dev. Neurosci. 2010; 28:195–205. [PubMed: 19913087]

Friedman LK, Avallone JM, Magrys B. Maturational effects of single and multiple early-life seizures on AMPA receptors in prepubescent hippocampus. Dev. Neurosci. 2007; 29:427–437. [PubMed: 17314473]

Friedman LK, Saghyan A, Peinado A, Keesey R. Age- and region-dependent patterns of Ca^{2+} accumulations following status epilepticus. Int. J. Dev. Neurosci. 2008; 26:779–790. [PubMed: 18687397]

Fuentes-Prior P, Salvesen GS. The protein structures that shape caspase activity, specificity, activation and inhibition. Biochem. J. 2004; 384(Pt 2):201–232. [PubMed: 15450003]

Geng JX, Cai JS, Zhang M, Li SQ, Sun XC, Xian XH, Hu YY, Li WB, Li QJ. Antisense oligodeoxynucleotides of glial glutamate transporter-1 inhibits the neuro-protection of cerebral ischemic pre-conditioning in rats. Sheng Li Xue Bao. 2008; 60:497–503. [PubMed: 18690392]

Gorter JA, van Vliet EA, Aronica E, Breit T, Rauwerda H, Lopes da Silva F, Wadman WJ. Potential new antiepileptogenic targets indicated by microarray analysis in a rat model for temporal lobe epilepsy. J. Neurosci. 2006; 26:11083–11110. [PubMed: 17065450]

Green JG, Borges K, Dingledine R. Quantitative transcriptional neuroanatomy of the rat hippocampus: evidence for wide-ranging, pathway-specific heterogeneity among three principal layers. Hippocampus. 2009; 19:253–264. [PubMed: 18830999]

Hansen MR, Roehm PC, Xu N, Green SH. Overexpression of Bcl-2 or Bcl-xL prevents spiral ganglion neuron death and inhibits neurite growth. Dev. Neurobiol. 2007; 67:316–325. [PubMed: 17443790]

Hara A, Iwai T, Niwa M, Uematsu T, Yoshimi N, Tanaka T, Mori H. Immunohistochemical detection of Bax and Bcl-2 proteins in gerbil hippocampus following transient forebrain ischemia. Brain Res. 1996; 711:249–253. [PubMed: 8680870]

Hatazaki S, Bellver-Estelles C, Jimenez-Mateos EM, Meller R, Bonner C, Murphy N, Matsushima S, Taki W, Prehn JH, Simon RP, Henshall DC. Microarray profile of seizure damage-refractory hippocampal CA3 in a mouse model of epileptic preconditioning. Neuroscience. 2007; 150:467–477. [PubMed: 17935890]

Haut SR, Velõsková J, Moshé SL. Susceptibility of immature and adult brains to seizure effects. Lancet Neurol. 2004; 3:608–617. [PubMed: 15380157]

Hebra A, Strange P, Egbert JM, Ali M, Mullinax A, Buchanan E. Intracellular cytokine production by fetal and adult monocytes. J. Pediatr. Surg. 2001; 36:1321–1326. [PubMed: 11528598]

Iacobas DA, Iacobas S, Urban-Maldonado M, Spray DC. Sensitivity of the brain transcriptome to connexin ablation. Biochim. Biophys. Acta. 2005; 1711:183–196. [PubMed: 15955303]

Iacobas DA, Iacobas S, Urban-Maldonado M, Scemes E, Spray DC. Similar transcri, ptomic alterations in Cx43 knock-down and knock-out astrocytes. Cell Commun. Adhes. 2008; 15:195–206. [PubMed: 18649190]

Iacobas S, Iacobas DA. Astrocyte proximity modulates the myelination gene fabric of oligodendrocytes. Neuron Glia Biol. 2011; 6:157–169. [PubMed: 21208491]

Inoue S, Browne G, Melino G, Cohen GM. Ordering of caspases in cells undergoing apoptosis by the intrinsic pathway. Cell Death Differ. 2009; 16:1053–1061. [PubMed: 19325570]

Jiang W, Van Cleemput J, Sheerin AH, Ji SP, Zhang Y, Saucier DM, Corcoran ME, Zhang X. Involvement of extracellular regulated kinase and p38 kinase in hippocampal seizure tolerance. J. Neurosci. Res. 2003; 81:581–588. [PubMed: 15948190]

Jimenez-Mateos EM, Hatazaki S, Johnson MB, Bellver-Estelles C, Mouri G, Bonner C, Prehn JH, Meller R, Simon RP, Henshall DC. Hippocampal transcriptome after status epilepticus in mice rendered seizure damage-tolerant by epileptic preconditioning features suppressed calcium and neuronal excitability pathways. Neurobiol. Dis. 2008; 32:442–453. [PubMed: 18804535]

Jones NM, Bergeron M. Hypoxia-induced ischemic tolerance in neonatal rat brain involves enhanced ERK1/2 signaling. J. Neurochem. 2004; 89:157–167. [PubMed: 15030400]

Kelly ME, McIntyre DC. Hippocampal kindling protects several structures from the neuronal damage resulting from kainic acid induced status epilepticus. Brain Res. 1994; 634:245–256. [PubMed: 8131074]

Kitagawa K, Matsumoto M, Kuwabara K, Tagaya M, Ohtsuki T, Hata R, Ueda H, Handa N, Kimura K, Kamada T. Ischemic tolerance' phenomenon detected in various brain regions. Brain Res. 1991; 561:203–211. [PubMed: 1802339]

Kondratyev A, Sahibzada N, Gale K. Electroconvulsive shock exposure prevents neuronal apoptosis after kainic acid-evoked status epilepticus. Brain Res. Mol. Brain Res. 2001; 91:1–13. [PubMed: 11457487]

Kutsuwada T, Kashiwabuchi N, Mori H, Sakimura K, Kushiya E, Araki K, Meguro H, Masaki H, Kumanishi T, Arakawa M, Mishina M. Molecular diversity of the NMDA receptor channel. Nature. 1992; 358:36–41. [PubMed: 1377365]

Laurén HB, Lopez-Picon FR, Brandt AM, Rios-Rojas CJ, Holopainen IE. Transcriptome analysis of the hippocampal CA1 pyramidal cell region after kainic acid-induced status epilepticus in juvenile rats. PLoS One. 2010; 5:e10733. [PubMed: 20505763]

Layé S, Parnet P, Goujon E, Dantzer R. Peripheral administration of lipopolysaccharide induces the expression of cytokine transcripts in the brain and pituitary of mice. Brain Res. Mol. Brain Res. 1994; 27:157–162. [PubMed: 7877446]

Liu H, Kaur J, Dashtipour K, Kinyamu R, Ribak CE, Friedman LK. Suppression of hippocampal neurogenesis is associated with developmental stage, number of perinatal seizure episodes, and glucocorticosteroid level. Exp. Neurol. 2003; 184:196–213. [PubMed: 14637092]

Liu H, Friedman LK, Kaur J. Perinatal seizures preferentially protect CA1 neurons from seizure-induced damage in prepubescent rats. Seizure. 2006; 15:1–16. [PubMed: 16309925]

Martinou JC, Subois-Dauphin M, Staple JK, Rodriguez I, Frankowski H. Overexpression of Bcl-2 in transgenic mice protects neurons from naturally occurring cell death and experimental ischemia. Neuron. 1994; 13:1017–1030. [PubMed: 7946326]

Najm IM, Hadam J, Ckakraverty D, Mikuni N, Penrod C, Christine S, Markarian G, Luders HO, Babb T, Baudry M. A short episode of seizure activity protects from status epilepticus induced neuronal damage in rat brain. Brain Res. 1998; 810:72–75. [PubMed: 9813246]

Nemethova M, Danielisova V, Gottlieb M, Kravcukova P, Burda J. Ischemic postconditioning in the rat hippocampus: mapping of proteins involved in reversal of delayed neuronal death. Arch. Ital. Biol. 2010; 148:23–32. [PubMed: 20426251]

Ogita K, Okuda H, Yamamoto Y, Nishiyama N, Yoneda Y. In vivo neuroprotective role of NMDA receptors against kainate-induced excitotoxicity in muring hippocampal pyramidal neurons. J. Neurochem. 2003; 85:1336–1346. [PubMed: 12753091]

Ortega A, Jadeja V, Zhou H. Postnatal development of lipopolysaccharide-induced inflammatory response in the brain. *Inflamm. Res.*. 2011; 60:175–185. [PubMed: 20865294]

Paxinos G, Watson CR, Emson PC. AChE-stained horizontal sections of the rat brain in stereotaxic coordinates. J. Neurosci. Meth. 1980; 3:129–149.

Popescu BO, Oprica M, Sajin M, Stanciu CL, Bajenaru O, Predescu A. Dantrolene protects neurons against kainic acid induced apoptosis in vitro and in vivo. J. Cell Mol. Med. 2002; 6:555–569. [PubMed: 12611640]

van Rensburg R, Errington DR, Ennaceur A, Lees G, Obrenovitch TP, Chazot PL. A new model for the study of high-K(+)-induced preconditioning in cultured neurones: role of N-methyl-d-aspartate and alpha7-nicotinic acetylcholine receptors. J. Neurosci. Meth. 2009; 177:311–316.

Represa A, Niquet J, Charriaut-Marlangue C, Ben-Ari Y. Reactive astrocytes in the kainic acid-damage hippocampus have the phenotypic features of type-2 astrocytes. J. Neurocytol. 1993; 22:299–310. [PubMed: 8478647]

Saghyan A, LaTorre GN, Keesey R, Sharma A, Mehta V, Rudenko V, Hallas BH, Rafiuddin A, Goldstein B, Friedman LK. Glutamatergic and morphological alterations associated with early life seizure-induced preconditioning in young rats. Eur. J. Neurosci. 2010; 32:1897–1911. [PubMed: 21050279]

Sedlak TW, Oltvai ZN, Yang E, Wang K, Boise LH, Thompson SB, Korsmeyer SJ. Multiple Bcl-2 family members demonstrate selective dimerization with Bax. Proc. Natl. Acad. Sci. 1995; 92:7834–7838. [PubMed: 7644501]

Semenov DG, Samoilov MO, Lazarewicz JW. Preconditioning reduces hypoxia-evoked alterations in glutamatergic Ca^{2+} signaling in rat cortex. Acta. Neurobiol. Exp. (Wars). 2008; 68:169–179. [PubMed: 18511953]

Sem'yanov AV, Morenkov ED, Godukhin OV. The decreased susceptibility to the development of in vitro kindling-like state in hippocampal CA1 slices of rats sensitive to audiogenic seizures. Neurosci. Lett. 1997; 230:187–190. [PubMed: 9272692]

Simpson PB, Challiss RA, Nahorski SR. Neuronal Ca^{2+} stores: activation and function. Trends Neurosci. 1995; 18:299–306. [PubMed: 7571010]

Soares MBP, Lima RS, Rocha LL, Vasconcelos JF, Rogatto SR, dos Santos RR, Iacobas S, Goldenberg RC, Iacobas DA, Tanowitz HB, Campos de Carvalho AC, Spray DC. Gene expression changes associated with myocarditis and fibrosis in hearts of mice with chronic chagasic cardiomyopathy. J. Infect. Dis. 2010; 202:416–426. [PubMed: 20565256]

Spray DC, Iacobas DA. Organizational principles of the connexin-related brain transcriptome. J. Membrane Biol. 2007; 218:39–47. [PubMed: 17657523]

Stewart CR, Landseadel JP, Gurka MJ, Fairchild KD. Hypothermia increases interleukin-6 and interleukin-10 in juvenile endotoxemic mice. Pediatr. Crit. Care Me. 2010; 11:109–116.

Strauss KI, Narayan RK, Raghupathi R. Common patterns of bcl-2 family gene expression in two traumatic brain injury models. Neurotox. Res. 2004; 6:333–342. [PubMed: 15545017]

Vallières L, Rivest S. Regulation of the genes encoding interleukin-6, its receptor, and gp130 in the rat brain in response to the immune activator lipopolysaccharide and the proinflammatory cytokine interleukin-1beta. J. Neurochem. 1997; 69:1668–1683. [PubMed: 9326296]

Wang Q, Yu S, Simonyi A, Rottinghaus G, Sun GY, Sun AY. Resveratrol protects against neurotoxicity induced by kainic acid. Neurochem. Res. 2004; 29:2105–2112. [PubMed: 15662844]

Ward NS, Waxman AB, Homer RJ, Mantell LL, Einarsson O, Du Y, Elias JA, Am J. Interleukin-6-induced protection in hyperoxic acute lung injury. Am. J. Resp. Cell Mol. 2000; 22:535–542.

Xu C, Bailly-Maitre B, Reed JC. Endoplasmic reticulum stress: cell life and death decisions. J. Clin. Invest. 2005; 115:2656–2664. [PubMed: 16200199]

Yang L, Li F, Zhang H, Ge W, Mi C, Sun R, Liu C. Astrocyte activation and memory impairment in the repetitive febrile seizures model. Epilepsy Res. 2009; 86:209–220. [PubMed: 19643577]

Yu S, Zhao T, Guo M, Fang H, Ma J, Ding A, Wang F, Chan P, Fan M. Hypoxic preconditioning upregulates glucose transport activity and glucose transporter (GLUT1 and GLUT3) gene expression after acute anoxic exposure in the cultured rat hippocampal neurons and astrocytes. Brain Res. 2008; 1211:22–29. [PubMed: 18474279]

Zimmermann C, Ginis I, Furuya K, Klimanis D, Ruetzler C, Spatz M, Hallenbeck JM. Lipopolysaccharide-induced ischemic tolerance is associated with increased levels of ceramide in brain and in plasma. Brain Res. 2001; 895:59–65. [PubMed: 11259760]

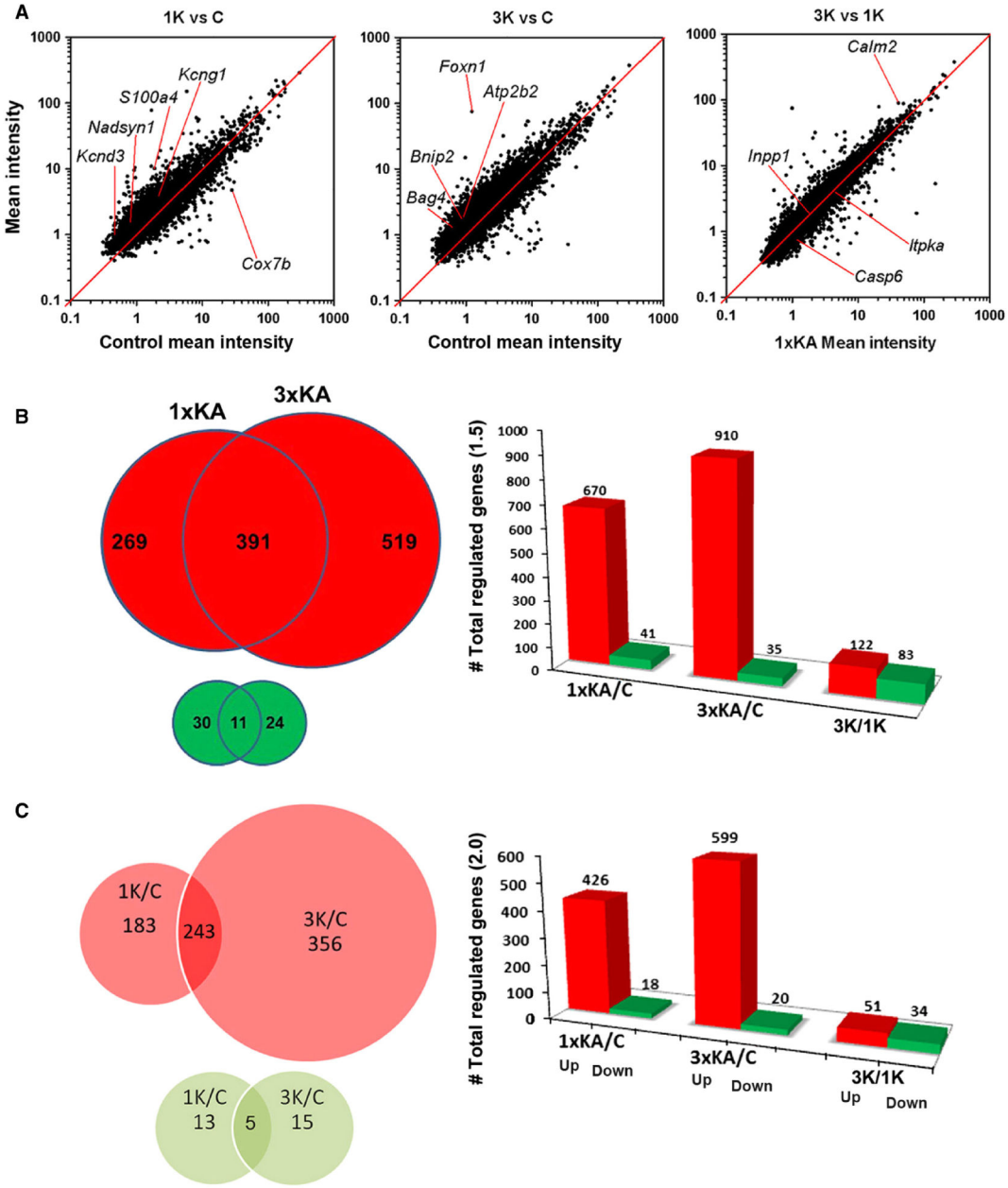

Fig. 1.

(A) Scatter diagrams of gene expression changes after single vs. multiple early-life seizures, following 1 × KA and 3 × KA with respect to control and following 3 × KA with respect to 1 × KA. The scatter plots show that more genes were upregulated than were downregulated, and that a unique set of genes were differentially regulated. The solid line is a line of equality ($x = y$) to the scatterplot with zero intercept. (B) Venn diagrams and bar graphs of the total number of genes regulated by ≥ 1.5-fold after 1 × KA vs. 3 × KA; $P < 0.5$. (C) Venn diagrams and bar graphs of the total number of genes regulated by ≥ 2-fold after 1 × KA vs. 3 × KA. The number of upregulated genes (large red circles) is significantly greater than the number of downregulated genes (small green circles).

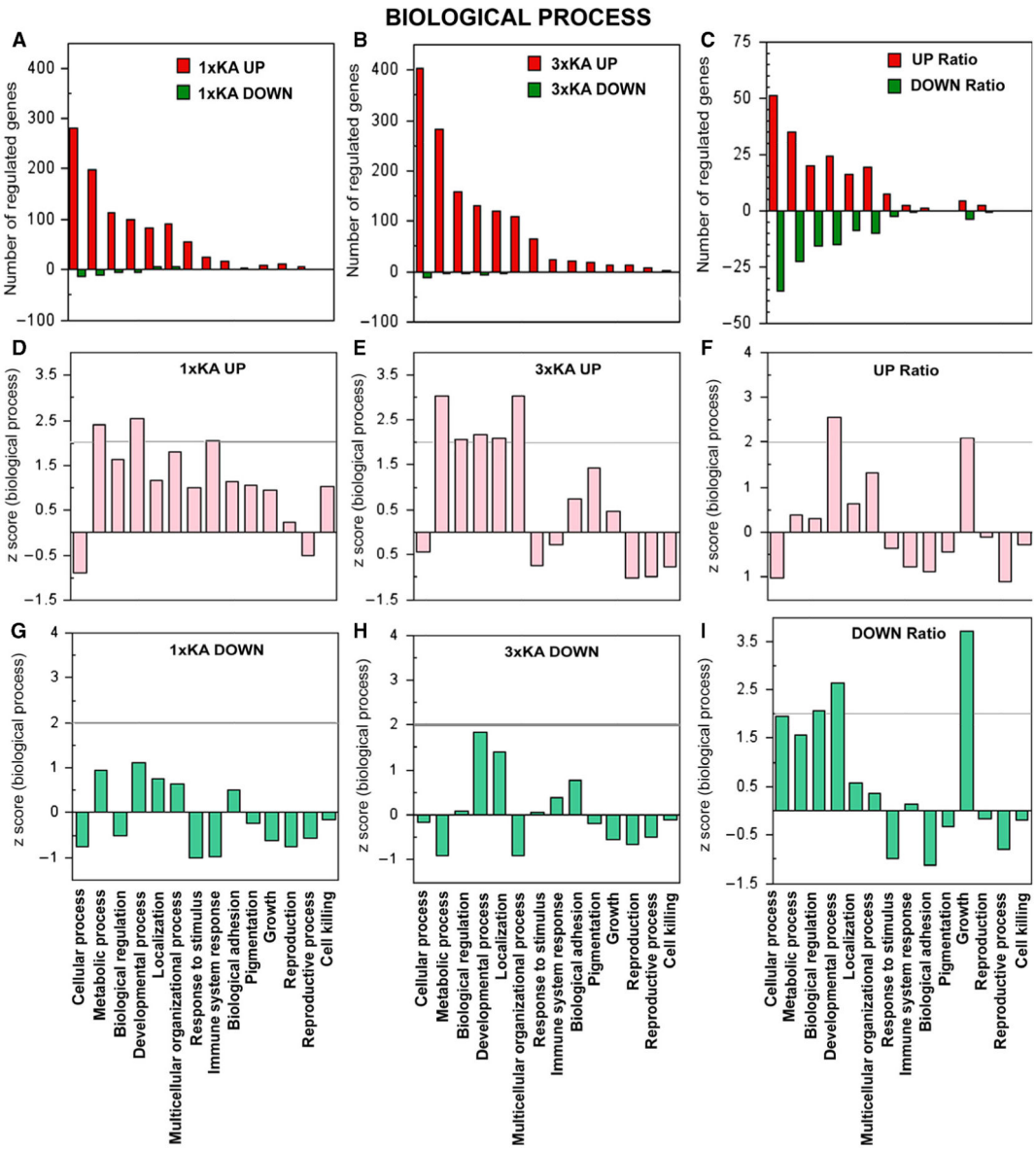

Fig. 2.

Ontology of genes regulated within biological process. (A–C) Bar graphs show number of genes (red) upregulated and (green) downregulated by ≥ 2-fold 72 h after status epilepticus. (A) 1 × KA vs. Control. (B) 3 × KA vs. Control. (C) 3 × KA vs. 1 × KA. (D–I) Graphs illustrate Z-scores (extent to which a certain function is significantly over- or under-represented) for genes up- or downregulated. (D) After 1 × KA, metabolic and developmental processes and immune system response were most over-represented. (E) After 3 × KA, metabolic, developmental processes and multicellular process were most over-represented. (F) The ratio revealed that differentially upregulated genes within developmental process and growth categories continued to be significant. (G and H) After 1 × KA or 3 × KA, downregulated genes did not reach statistical significance within any

category of biological process. (I) The ratio revealed differentially downregulated genes under biological regulation, developmental process and growth.

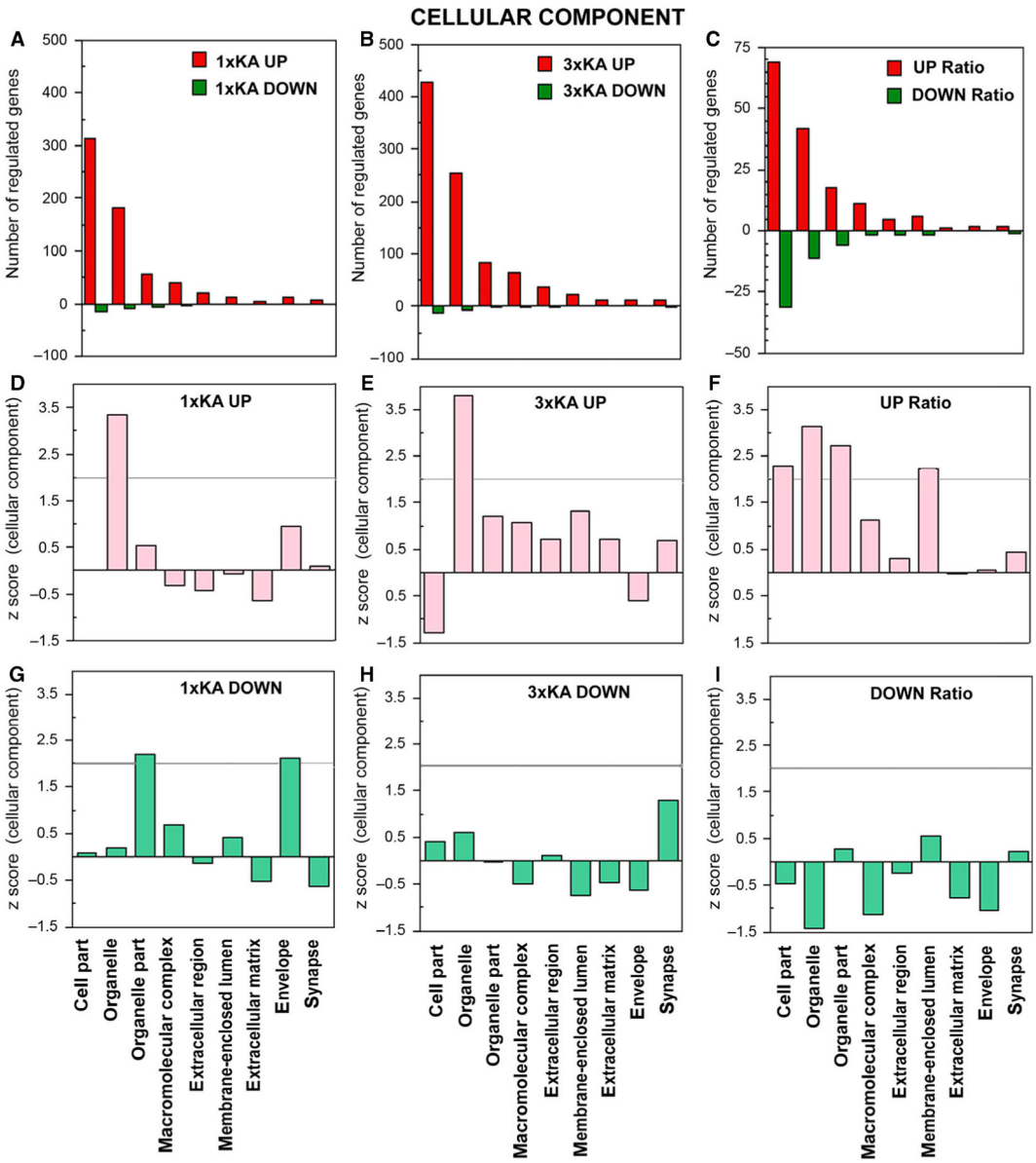

Fig. 3.

Ontology of genes regulated within cellular components. (A–C) Bar graphs show number of genes up- or downregulated by ≥ 2-fold 72 h after status epilepticus, with and without a history of two neonatal seizures. (A) 1 × KA vs. Control. (B) 3 × KA vs. Control. (C) 3 × KA vs. 1 × KA. (D and E) Graphs show that the only significant positive Z-score was found within the organelle category following either 1 × KA or 3 × KA. (F) The ratio revealed differentially upregulated genes within cell part, organelle and organelle part, and membrane-enclosed lumen. (G) After 1 × KA, significant positive Z-scores among downregulated genes were found within the categories organelle part and envelope. (H and I). No significant Z-scores for downregulated genes were observed under this ontology after 3 × KA or after calculating the ratio of 3 × KA/1 × KA.

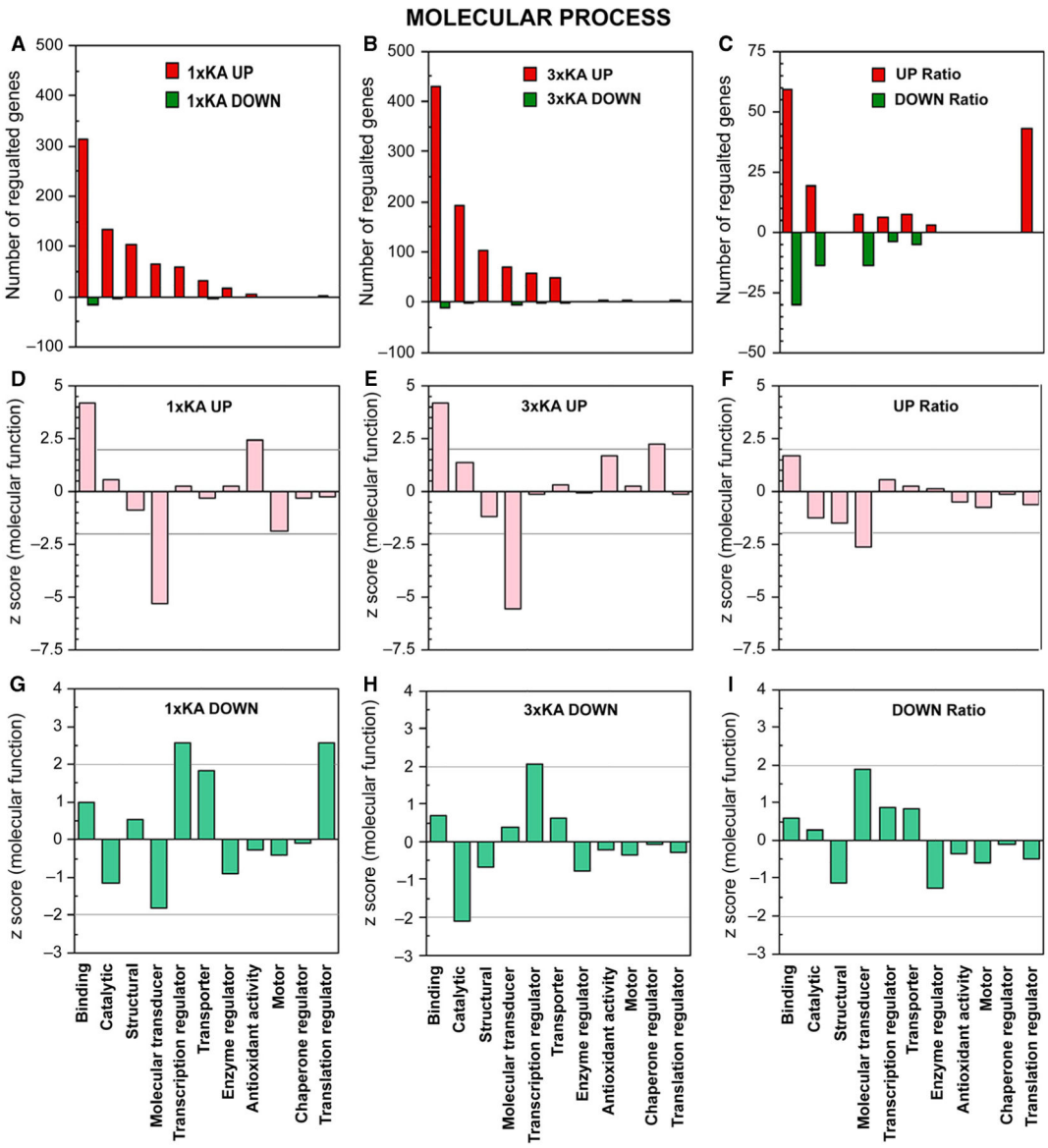

Fig. 4.

Ontology of genes regulated within molecular process. Bar graphs show number of genes upregulated (red) or downregulated (green) by ≥ 2-fold 72 h after status epilepticus, with and without a history of two neonatal seizures. (A–C) Bar graphs show number of genes up- or downregulated by ≥ 2-fold 72 h after status epilepticus, with and without a history of two neonatal seizures. (A) 1 × KA vs. Control. (B) 3 × KA vs. Control. (C) 3 × KA vs. 1 × KA. (D and E) After 1 × KA or 3 × KA, graphs show that binding and antioxidant activity were over-represented and molecular transducer was significantly under-represented. (E) After 3 × KA, genes within chaperone regulator were increased. (F) In the calculated ratio, no genes were differentially regulated within this ontology. (G) After 1 × KA, the highest positive Z-scores for downregulated genes were found within transcription regulator and translation regulator. (H) After 3 × KA, genes were only observed within transcription regulator. (I) The calculated ratio revealed only a trend within molecular transducer.

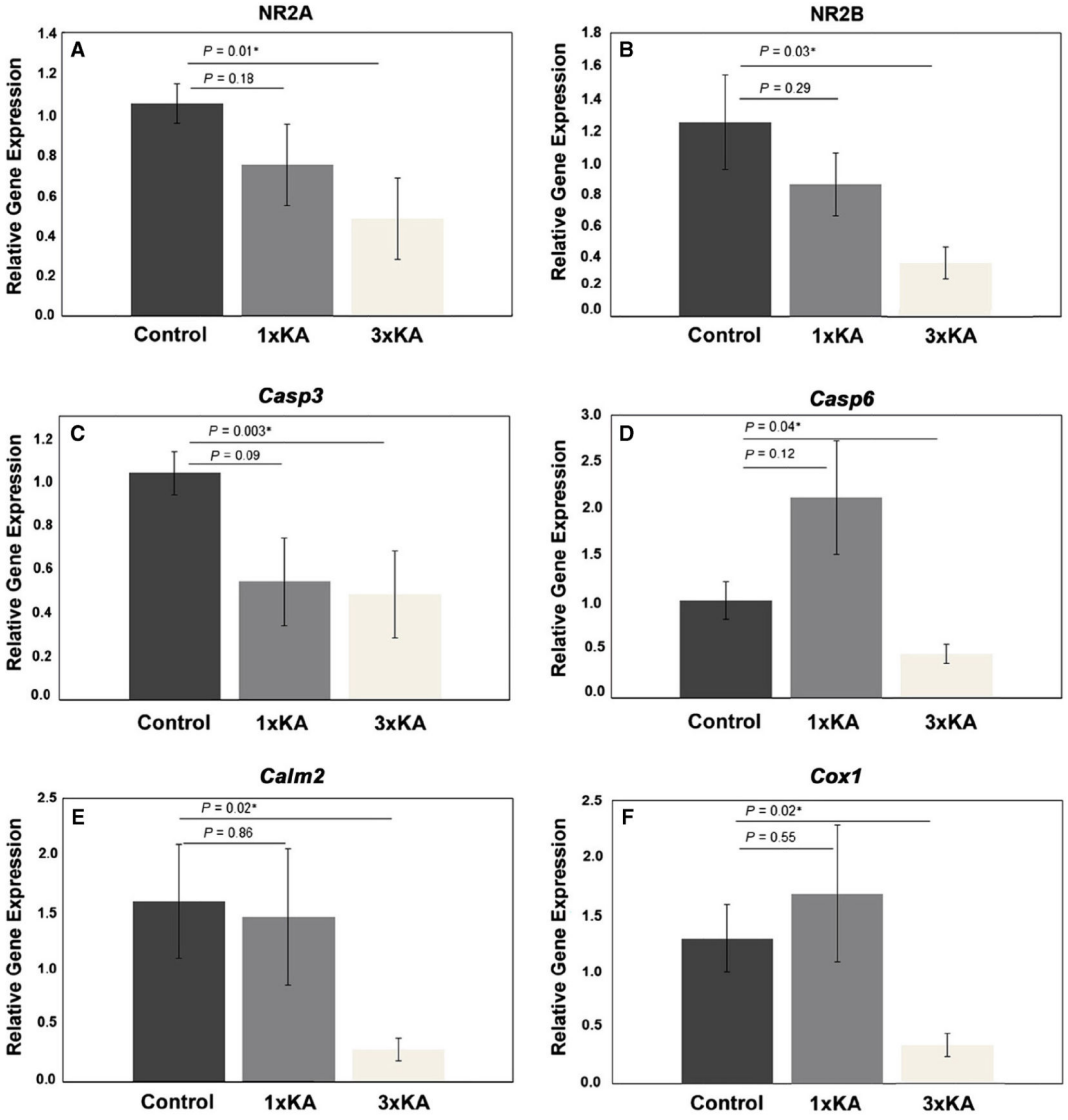

Fig. 5.

QPCR-findings of changes in relative gene expression in CA1 (P20) after 1 × KA or 3 × KA. Experimental samples were compared to corresponding tissues from untreated controls. Significant treatment effects on the expression of the NMDA receptors (A) *NR2A* and (B) *NR2B*, as well as (C) *Casp3*, (D) *Casp6*, (E) *Calm2* and (F) *Cox1* are depicted. Values are means ≥ SEM. *$P < 0.05$; $n = 7$.

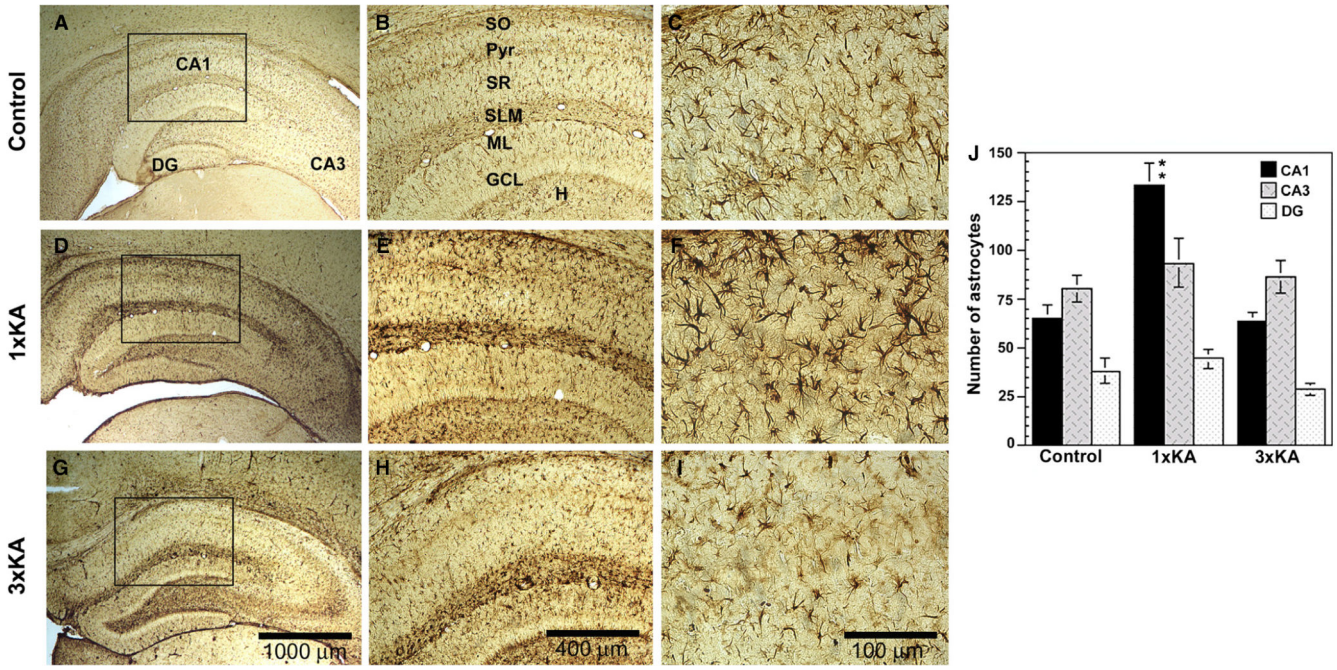

Fig. 6.

Photomicrographs of GFAP immunohistochemistry at 72 h after one or three episodes of status epilepticus. (A–C) In controls, glial cells were star-like in appearance with thin fibers; staining was light and uniform across the hippocampal subfields with the highest density being outside the principle cell layers, in structures such as the hilus, stratum radiatum and stratum lacunosum moleculare; three magnifications are shown (*box*). (D–F) After 1 × KA, there was an increase in GFAP staining throughout the subfields. Astrocytes appeared to increase in the CA1 and many changed in appearance; they were very dark with thick stubby projections (visible at 400× magnification). (G–I) After 3 × KA, astrocytic labeling in the CA1 subregion appeared similar to controls but other subregions resembled KA-treated animals. (J) Graphic analysis of the number of astrocytes in the hippocampus after multiple seizures showed that the number of astrocytes significantly increased in the CA1 by two-fold after 1 × KA but was attenuated after 3 × KA. Results are expressed as means ± SEM of 4–6 animals per group; $^{**}P < 0.05$.

Table 1

Common genes downregulated, identified under two criteria: ≥ 1.5 ×* and ≥ 2.0 ×**

Gene	Symbol	1K/C	3K/C	Biological description
Alpha-2-glycoprotein 1, zinc*	Azgp1	−1.84	−2.43	Lipolysis, lung secretion
Calmin*	Clmn	−1.84	−2.0	Development, growth
Clusterin-like 1 (retinal)**	Clul1	−2.253	−3.34	Cell death cones: acts as a pro-death signal, inhibiting cell growth and survival
Coiled-coil domain-containing 40**	Ccdc40	−2.185	−3.15	Mitochondria transport: assembly of dynein regulatory complex (DRC) and inner dynein arm complexes, which are responsible for ciliary beat regulation
FLT3-interacting zinc finger 1*	Fiz1	−1.83	−1.94	Tyrosine kinase, photoreceptors
Myosin binding protein H*	Mybph	−1.79	−1.69	Muscle activity
Paired-like homeodomain transcription factor 2*	Pitx2	−1.77	−1.88	Heart development
Rhesus blood group-associated A glycoprotein**	Rhag	−2.58	−3.87	Associated with rhesus blood group antigen expression; transport or channel function in the erythrocyte membrane
S100 calcium binding protein A5**	eS100a5	−4.73	−3.87	Cell cycle differentiation exocytosis and endocytosis; stimulation of Ca^{2+}-induced Ca^{2+} release, and implicated in the transportation of proteins involved in mood regulation, nociception and cell polarisation
T-box 2*	Tbx2	−1.87	−2.66	Group of transcription factors involved in limb and heart development
Transmembrane protein 138**	Tmem 138	−2.636	−3.95	Mutation leads to ciliary dysfunction and Joubert Syndrome (absence or underdevelopment of the cerebellar vermis, an area of the brain that controls balance and coordination)

1K/C, ratio of 1 × KA to control values; 3K/C, ratio of 3 × KA to control values.

Note that the negative signs indicate downregulation; −X/C for each experimental group. For example, −1.84 indicates 1.84× fold reduction in intensity values compared to control.

* Genes identified from a 1K/C ratio exceeding −1.5.

** Genes identified from a 1K/C ratio exceeding −2.0.

Table 2

Genes uniquely downregulated (uncommon) after 1 × KA

Gene	Symbol	1K/C	Biological process
Calmodulin 2	Calm2	−2.455	Regulation of Ca^{2+} transducion of Ca^{2+} signals by binding Ca^{2+} ions and then modifying its interactions with various target proteins
Cytochrome c oxidase subunit VIIb	Cox7b	−5.97	A terminal component of the mitochondrial respiratory chain
Integrator complex subunit 10	Ints10	−3.602	Involved in the small nuclear RNAs (snRNA) U1 and U2 transcription
Lipoprotein lipase	Lpl	−2.926	Hydrolysis of triglycerides of circulating chylomicrons
Myeloid leukemia factor 1 interacting protein	Mlf1ip	−2.343	Encodes for a putative transcriptional repressor
Numb-like	Numbl	−2.100	Negative regulator of NF-kappa-B signaling pathway, and neurogenesis
Olfactomedin 2	Olfm2	−2.102	Encodes Noelin-2 protein
Olfactory receptor 1225	Olr1225	−2.791	Encodes a protein that exhibits olfactory receptor activity
Solute carrier family 25 (mitochondrial carrier; adenine nucleotide translocator), member 4	Slc25a4	−2.958	Involved with oxidative phosphorylation
Tyrosine 3-monooxygenase/tryptophan 5-monooxygenase activation protein, epsilon polypeptide	Ywhae	−2.145	Regulation of highly conserved proteins (metabolism, trafficking, transduction)
UDP-Gal:betaGlcNAc beta 1,4-galactosyltransferase, polypeptide 6	B4galt6	−2.567	Exclusive specificity for the donor substrate UDP-galactose
UDP-N-acetyl-alpha-Dgalactosamine: polypeptide N-acetylgalactosaminyltransferase 9	Galnt9	−2.308	Transfer of an N-acetyl-Dgalactosamine residue to a serine or threonine residue
Wolfram syndrome 1 homolog (human)	Wfs1	−2.975	Regulation of Ca^{2+} for homeostasis

Genes were identified based on the value 1K/C exceeding −2.0 (the negative sign indicates downregulation). 1K/C, ratio of 1 × KA to control values.

Table 3

Genes uniquely downregulated (uncommon) after 3 × KA

Gene	Symbol	3K/C	Biological process
Alpha-2-glycoprotein 1, zinc	Azgp1	−2.435	Negative regulation of proliferation, immune response, lipid catabolism
ATPase, class VI, type 11A	Atp11a	−3.050	Phosphorylation drives the transport of ions such as Ca^{2+} across membranes
Calmin	Clmn	−2.085	Calponin-like transmembrane domain protein
Cholinergic receptor, nicotinic, alpha polypeptide 1 (muscle)	Chrna1	−3.599	Defect causes myasthenic syndrome slow-channel type
Growth differentiation factor 15	Gdf15	−2.047	Regulates inflammatory and apoptotic pathways in disease processes
Malate dehydrogenase 1B, NAD (soluble)	Mdh1b	−2.447	Putative malate dehydrogenase mitochondrial respiration
NK2 transcription factor related, locus 9 (Drosophila)	Nkx2-9	−2.57	Involved in axonogenesis and lung development; negative regulation of epithelial cell proliferation
Olfactory receptor 625	Olr625	−2.020	G-protein-coupled receptor signalling pathway for smell
Protein tyrosine phosphatase, receptor type, f polypeptide (PTPRF), interacting protein (liprin), alpha 2	Ppfia2	−2.767	Liprins interact with members of LAR family of transmembrane protein tyrosine phosphatases, which are known to be important for axon guidance and mammary gland development
Rho guanine nucleotide exchange factor (GEF) 4	Arhgef4	−3.425	Fundamental role in numerous cellular processes that are initiated by extracellular stimuli that work through G-protein-coupled receptors
SCY1-like 2 (*Saccharomyces cerevisiae*)	Scyl2	−2.100	Regulate clathrin-dependent trafficking between the TGN and/or the endosomal system
Solute carrier family 45, member 3	Slc45a3	−2.214	Marker for prostate cells
T-box 2	Tbx2	−2.659	Group of transcription factors involved in limb and heart development
T-box 5	Tbx5	−2.200	transcriptional regulation of genes required for mesoderm differentiation
Tubulin cofactor a	Tbca	−2.076	Tubulin-folding protein

Genes were identified based on the value 3K/C exceeding −2.0 (negative values indicate downregulation). 3K/C, ratio of 3 × KA to control values.